

Performance Analysis and Mission Applications of a New Solar Sail Concept Based on Crossed Booms with Tip-Deployed Membranes

Patric Seefeldt^{a,*}, Jan Thimo Grundmann^a, Martin Hillebrandt^b, Martin Zander^b

^aInstitute of Space Systems, German Aerospace Center (DLR), 28359 Bremen, Germany

^bInstitute of Composite Structures and Adaptive Systems, German Aerospace Center (DLR), 38108 Braunschweig, Germany

Abstract

For precursor solar sail activities a strategy for a controlled deployment of large membranes was developed based on a combination of zig-zag folding and coiling of triangular sail segments spanned between crossed booms. This strategy required four autonomous deployment units that were jettisoned after the deployment is completed. In order to reduce the complexity of the system an adaptation of that deployment strategy is investigated.

A baseline design for the deployment mechanisms is established that allows the deployment actuation from a central bus system in order to reduce the complexity of the system. The mass of such a sail craft will be slightly increased but its performance is still be reasonable for first solar sail missions.

The presented design will be demonstrated on breadboard level showing the feasibility of the deployment strategy. The characteristic acceleration will be evaluated and compared to the requirements of certain proposed solar sail missions.

Keywords: Solar Sails, Deployment Strategy, Deployable Membranes, Deployable Booms

Nomenclature

		γ	Area mass
A	Sail area	μ	Sail efficiency
L	Boom length	σ_{Sail}	Sail center stress
P	Sail tension load		
a_c	Characteristic acceleration		
f	Frequency		
k	Width of central spacecraft		
k_{FS}	Safety factor against buckling		
m	Mass		
p	Radiation pressure		
s	Sail edge length		
t_{Sail}	Sail thickness		
w	Width of foil sheet		
α	Outer angle of triangular sail segments		
β	Inner angle of triangular sail segments		

1. Introduction

The German Aerospace Center (DLR) can look back to a history of 20 years solar sail technology development (see Grundmann et al. (2019c)). From 2010 to 2016 this development was carried out in the Gossamer-1 project as presented by Seefeldt et al. (2017). Within this activity a deployment strategy was implemented based on four autonomous deployment units that, during deployment, move away from the central spacecraft bus unit. The system is based on a crossed boom configuration with four triangular sail segments. This process is illustrated in Figure 1. The development was aiming to achieve a design of large lightweight sails up to 40 m × 40 m that can be safely deployed in a controlled manner. In this context it must be taken into account that the deployment of the smaller 5 m × 5 m Gossamer-1 demonstrator took already more than 30 minutes and a deployment of a large sail would take several hours.

*Patric Seefeldt, patric.seefeldt@dlr.de

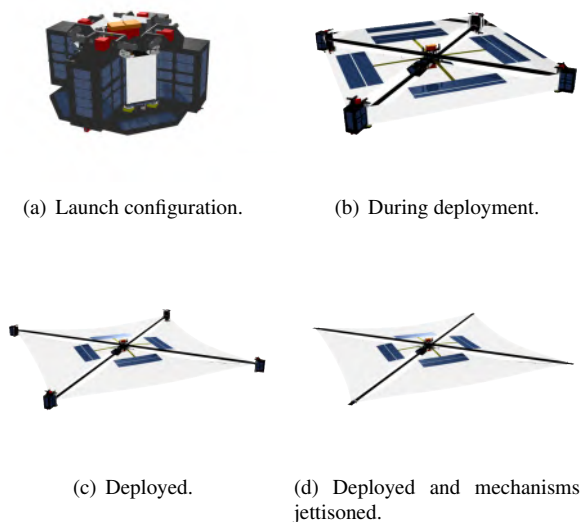


Figure 1: Gossamer-1 stowing strategy and deployment sequence.

This is mostly due to technical limits of actuators like electrical motors which have to be tightly controlled and synchronized to ensure that the membrane is not torn and the long booms do not buckle under temporary asymmetric load spikes. With the Gossamer-1 deployment strategy the controlled deployment is achieved by ensuring three major points:

- the membrane is slightly tensioned throughout the deployment process and can not become entangled with other components,
- the booms can be properly mounted (independent from the deployment mechanism) on to the spacecraft so that they can provide sufficient stability also during the deployment,
- all mechanisms required for the deployment are jettisoned, leaving only the lightweight sailcraft for the solar sail mission.

While this strategy achieves the best performance parameters it has one disadvantage. For developments in low funded projects with very limited resources the complexity is relatively high. Each of the deployment units has a complexity comparable to a small CubeSat with several subsystems beside the deployment mechanisms itself. It requires power, communication, an on-board computer and data handling as well as a structural and thermal design that has to function in very different configurations (undeployed, during deployment and deployed).

The work presented here studies an implementation of the deployment strategy without employing the described independent deployment units. Instead, the deployment is driven from a central unit and only the sail spools, which are passive elements, are mounted to the boom tips. By deploying the booms from the central unit, the spools mounted to the boom tips move away from the central unit and the sail membranes are pulled off of the spool. The principle design is shown in Figure 2. While this reduces the complexity, it comes at the expense of additional mass and thus a reduction of sail craft performance. Sections 2 and 3 describe the implications on the membrane and boom deployment. Deployment tests are shown in Section 4 followed by an estimation of the solar sail performance and an investigation of possible missions feasible with this performance in Section 5.1.

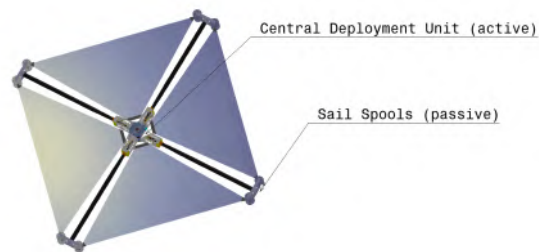


Figure 2: Deployment with central deployment unit and sail spools mounted to the tip of the booms.

2. Membrane stowing and deployment

Taking into account that the sail should be tensioned throughout the deployment process and using a crossed boom configuration with triangular sail segments, it is necessary to deploy the full length of the hypotenuse at the end of the deployment process. This leads to a strategy which coils the folded sail segments on two spools, starting from the outer edges (see Figure 3). The triangular segments are first zig-zag folded and then coiled onto two spools. Seefeldt (2017) described the stowing strategy with a mathematical model.

The sail is coiled onto two spools. Instead of mounting the spools to the deployment units, as considered in the original Gossamer-1 concept, the spools are mounted directly to the boom tips. Figure 4 shows the spool assembly. During the deployment the spools can rotate on plain bearings thereby releasing the folded and coiled sail segments. In order to keep the sail slightly tensioned during the deployment and prevent a premature uncoiling due to elastic energy, the spools rotate



Figure 3: Membrane stowing strategy. As considered in previous concepts, the figure also shows flexible photovoltaic mounted close to the central unit.

against a brake torque. The brake is constructed out of two copper beryllium blades that engage into a gear that is part of the spool. The deflection of the spring blades lead to an oscillating force or torque, respectively. Using two blades gives more flexibility in adjusting the brake torque and the oscillations are evened out to a certain extent.

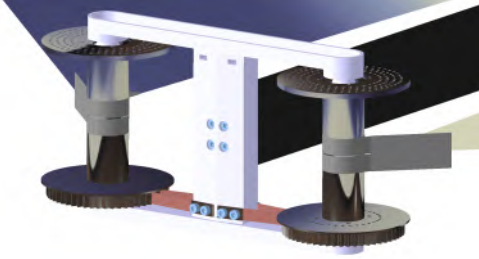


Figure 4: Membrane spool assembly.

The membrane consists mainly of a thin film. Most of projects currently consider coated polyimide membranes. The available products are delivered on a roll with limited width. Within DLR's Gossamer-1 project the material Upilex-S with a 100 nm aluminium was considered. The materials density is about 1350 kg/m^3 and the width of the foil w is 1.016 m. The sail membranes are built by bonding several sheets together, cutting out the desired geometry and reinforcing edges and interface points. Bond lines used 3M Tape 966 with adhesive 100, which has a mass of about 0.6 g/m for a tape of 1.27 cm width. For a simplified mass estimation for different sail size the geometry as shown in Figure 5 is used considering $k = 0.34 \text{ m}$. The sail area is calculated as

$$A = 4 \cdot \frac{s}{2} \cdot \frac{s-k}{2} . \quad (1)$$

The angles are given by

$$\alpha = \tan^{-1} \left(\frac{s}{s-k} \right) , \quad (2)$$

and

$$\beta = \frac{\pi - \alpha}{2} . \quad (3)$$

This yields the membrane masses shown in Figure 6.

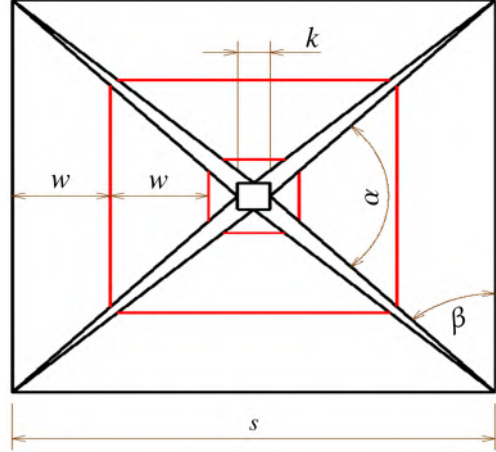


Figure 5: Simplified sail geometry for mass estimation, bonding lines of the foil sheets are shown in red.

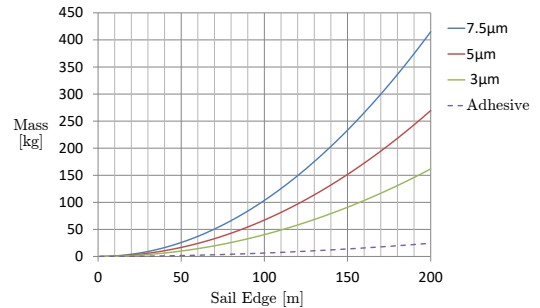


Figure 6: Mass of the membrane for different thickness of polyimide and mass of adhesive.

3. Boom and boom deployment

The deployment of the sail quadrants is driven by a central deployment unit that simultaneously unfolds the four tubular booms and thereby also the sail segments that are attached to their tips. The design of the booms, the deployment unit and their scaling behaviour in a solar sail application are described in the following.

3.1. Boom design

The booms displayed in Figure 7(a) are tubular masts of lenticular shape and are described in several publications such as Rubin (1969), Sickinger (2009) and Hillebrandt et al. (2014). They are composed of thin-walled shells made of a flexible carbon fiber composite material that enables high degrees of elastic deformation. In combination with the lenticular cross-sectional shape the booms can be folded to a flat band that is reeled on a cylinder. The thereby elastically stored strain energy is used to regain the original shape during the deployment process. However, means to control the release of the strain energy are required to avoid a chaotic boom deployment (see Sickinger (2009)). A controlled boom deployment is achieved through the according control and regulation functionalities provided by the deployment unit.



(a) Reelable, tubular double-omega boom in partly deployed state. (b) Breadboard model of the boom deployment unit with four cross-wise aligned booms.

Figure 7: Boom and deployment mechanism.

3.2. Deployment unit design

The design of the deployment unit displayed in Figure 7(b) depends primarily on the stowed form and deployment principle of the booms. The central component is a cylindrical spool that contains all four stowed masts. Adjacent to this spool are four, cross-wise aligned arms oriented along the deployment directions which support the booms during their transition from the flattened to the deployed state. The deployment of the booms is achieved through four co-coiled steel belts that enable introduction of the deployment forces into the thin walled booms. Such a concept is described in further detail in Seefeldt et al. (2017); Hillebrandt and Zander (2018); Hillebrandt (2019). Therefore the steel belts are set under tension through coiling them on separate spools whereby they simultaneously pull the booms off the spool.

A unique feature of the deployment unit is the so-called “sliding core interface” which is located at the ends of each support arm and enables a high stiffness and good load transmission between the booms and the

deployment unit. It is based on a core that is sliding inside the fully closed boom and is held contactless in position by a surrounding cage. Thereby the cage and the sliding core form an interface similar to an extrusion nozzle that constraints load induced movements and deformations of the boom shell to a minimum. Hillebrandt et al. (2019) described the design of this interface in more detail.

3.3. Scaling functions of booms and central deployment unit

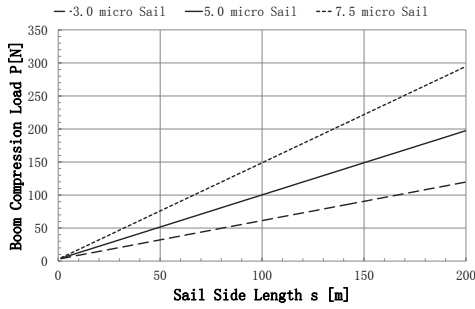
Of primary interest for a solar sail is how its mass scales with its size and mission requirements as the mass is a direct measure for its propulsion efficiency. For the derivation of according mass scaling functions, a mission in the vicinity of the Earth’s orbit is assumed. Here, the compression loads on the booms from sail tension forces are dominating and bending loads from solar pressure are relatively low. Hence, the load case for scaling of the booms is axial compression due to sail tensioning. The required sail tension load P is calculated according to Murphey (2006) and Greschik et al. (2003) as

$$P = k_{FS} \sigma_{Sail} t_{Sail} L \quad (4)$$

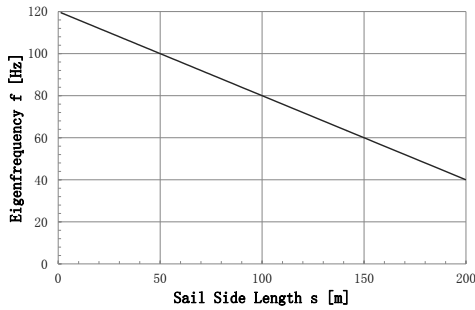
It depends on the required sail center stress σ_{Sail} , the sail thickness t_{Sail} , the boom length L and a safety factor k_{FS} against buckling. In the following calculations, the sail center stress is set to 91.7 kPa in accordance with Greschik et al. (2003). It also avoids multiple reflections in folding lines and the corresponding temperature increase as described in Seefeldt and Dachwald (2021). The sail thickness is varied between $3 \mu\text{m}$, $5 \mu\text{m}$ and $7.5 \mu\text{m}$ and the buckling safety factor is set to 3. The corresponding boom compression loads are displayed in Figure 8(a).

The scaling functions for the thin-walled and slender booms corresponding to this load case are developed from constraint functions on global column buckling and local wall buckling. Implemented in the functions is the reduced stiffness and load carrying capability of the boom within its transition zone as it is not fully enclosed by the support arms of the deployment unit. Hillebrandt and Zander (2018) describe considerations associated with this transition zone in tubular shell masts. Of high importance for the formulation of the scaling functions are constraints set by scaling limits particularly in the small scale region. Such limits for the tubular shell booms are a minimum wall thickness and strain limits of the shell material during folding.

The scaling functions for the components of the deployment unit possess a high dependency on those of



(a) Design compression loads for the booms plotted over the sail edge length for sail thicknesses of $3\ \mu\text{m}$, $5\ \mu\text{m}$ and $7.5\ \mu\text{m}$.



(b) Design eigenfrequency requirement for the stowed system during space transport plotted over the sail edge length.

Figure 8: Compression load and eigenfrequency considerations for the scaling functions of the boom and its deployer.

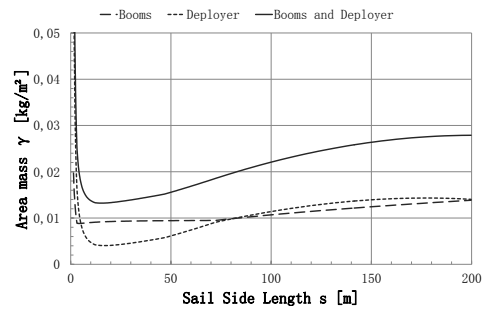
the booms as their stowed form and size determine the deployment unit's form and size. The according scaling functions are developed from constraint functions resulting from functional requirements such as providing a certain deployment force and requirements set by the transport into space. The latter are considered by a minimum fundamental frequency and a lateral acceleration load the stowed system has to comply with. Particularly sensitive is the mass of the deployment unit towards the fundamental frequency requirement. As in general the frequency requirement is inversely proportional to the spacecraft mass, the requirement is reduced with increasing sail size according to Figure 8(b). Within the deployment unit scaling functions, scaling functions for each component individual are considered.

A detailed presentation of the underlying scaling functions for booms and deployment unit is beyond the scope of this paper and is further described by Hille-

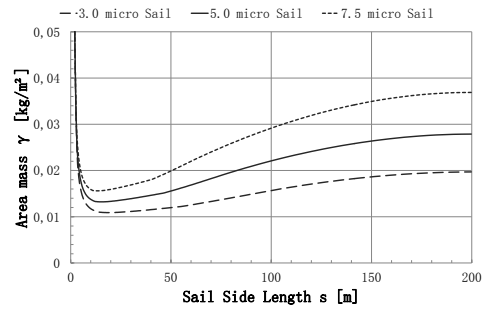
brandt (2019).

3.4. Boom deployment system scaling behaviour

The mass scaling results of the booms, the deployment unit and their combined mass are displayed in Figure 9(a) for a sail membrane with a thickness of $5\ \mu\text{m}$. The mass values are given normalized by the corresponding sail area to gain an application related measure for the mass efficiency of booms and deployment unit. The resulting mass per unit area γ is thereby plotted over the sail side length s .



(a) Mass per unit area of the booms, the boom deployment unit and the combined parts plotted over the sail edge length.



(b) Influence of the sail thickness on the combined mass per unit area of booms and deployment unit for sail thicknesses of $3\ \mu\text{m}$, $5\ \mu\text{m}$ and $7.5\ \mu\text{m}$.

Figure 9: Mass scaling results for the boom and the deployer.

The curves show in the small scale region a rapidly decreasing mass per unit area with increasing sail side length down to a minimum of $13.2\ \text{gm}^{-2}$ around 20 m (combined) followed by an increase for larger sails. The initial decay is caused by scaling limits of the booms and the deployment unit. Many dimensions such as the boom cross-section reach practical limits wherefore

component masses become overly heavy in comparison to the sail size. The various scaling limits cause change-overs in the scaling functions which are visible in the curves of booms and deployment unit in the form of discontinuities. In the large scale region particularly the deployment unit causes the increase in the mass per unit area. This is partly due to the fact that architectural parameters such as face-sheet thickness ratios of the support structure components are selected for the small to mid-size region and are not adjusted accordingly throughout the observed size interval. Hence the gradient of the increase in mass per unit area for large sails may be lowered through proper adjustment of these architecture parameters. However, as the curve of the also increasing boom mass scaling function shows, the general trend still remains the same. Here means to reduce the boom loading for larger sails may be promising to limit this effect.

Figure 9(b) shows the influence of the sail thickness on the mass efficiency of the booms and the deployment unit. As the sail tension forces scale with the sail thickness, a reduction also causes a decrease in the boom compression loads. The impact of this decrease on the boom and deployment unit masses is significant. Reducing the sail thickness from $7.5\ \mu\text{m}$ to $3\ \mu\text{m}$ lowers the combined minimum mass per unit area of booms and deployment unit by 30 % from $15.6\ \text{gm}^{-2}$ at 14 m to $10.9\ \text{gm}^{-2}$ at 20 m sail side length. For a sail side length of 200 m the mass per unit area decreases from $36.9\ \text{gm}^{-2}$ to $19.7\ \text{gm}^{-2}$ which corresponds to an improvement of 47 %.

4. Breadboard functional tests

The design as described was implemented on breadboard level in order to verify the functional principles of the deployment mechanism as well as the deployment strategy itself. The breadboard sail segments are downscaled with an edge length of 1.4 m. The booms and the deployment drive could in principle deploy a sail area of about $10\ \text{m} \times 10\ \text{m}$. Figure 10 gives an impression of the breadboard sail. The deployment was smooth without any unexpected events. It should be stated that in contrast to the previous design the tests on ground are more easy to implement. This is because there is no need to support relatively heavy deployment units during a test which is difficult to do without introducing loads that are purely test related. In addition there is no relative movement between the membrane and the supporting test structure underneath. This is often the case for other deployment strategies and leads to additional deployment loads during an on-ground deployment test

due to friction between the membrane and the supporting structure. However it remains challenging, even for a small sails, to test these structures under gravity.

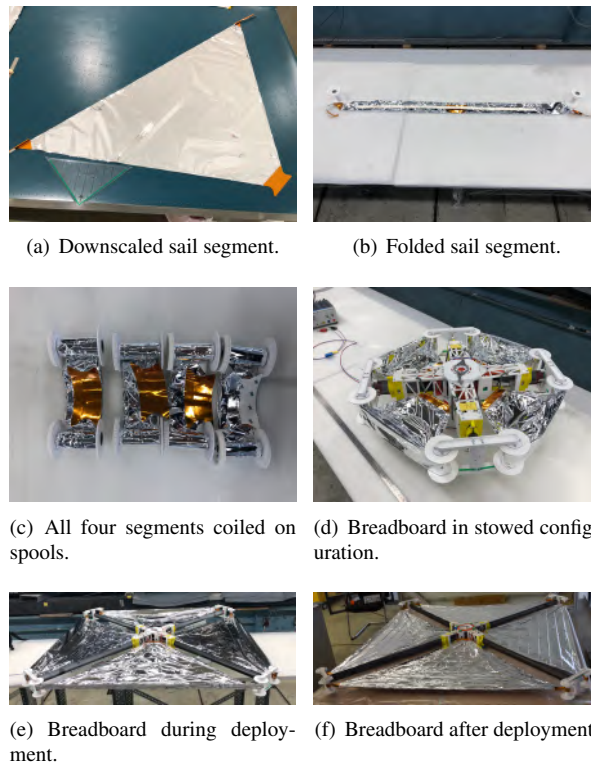


Figure 10: Breadboard sail with deployment drive, booms and down-scaled sail segments.

5. Results

5.1. Performance estimation

In order to estimate the characteristic acceleration achievable with the presented design concept, scaling of the technology needs to be taken under consideration for the mass budget. Based on the mass estimation described in Sections 2 and 3 the characteristic acceleration is calculated as

$$a_c = \frac{2\mu p}{\frac{m_{sail}}{A} + \frac{m_{S/C}}{A}} \quad (5)$$

Here μ is the sail efficiency, p is the radiation pressure and A is the sail area. For the evaluation of the characteristic acceleration it is differentiated between the sail mass m_{sail} and the mass added for the spacecraft systems and payload $m_{S/C}$. The characteristic acceleration is evaluated for two cases shown in Figure 11. The first

is for Gossamer-1 with deployment units that can be jettisoned (dashed lines in Figure 11). This results in a sail craft that does not include any mechanism mass. The second is for the here studied adaptation with a central deployment unit that cannot be jettisoned (solid lines in Figure 11). In addition Figure 11 shows the characteristic acceleration of the sail with booms and membrane only (blue dotted line), and of the sail with the central deployment unit (red dotted line). In all cases a $5\mu\text{m}$ thick sail membrane with a efficiency μ of 0.9 is considered. The radiation pressure p at 1 AU (without reflection) is $4.575\mu\text{Nm}^{-2}$.

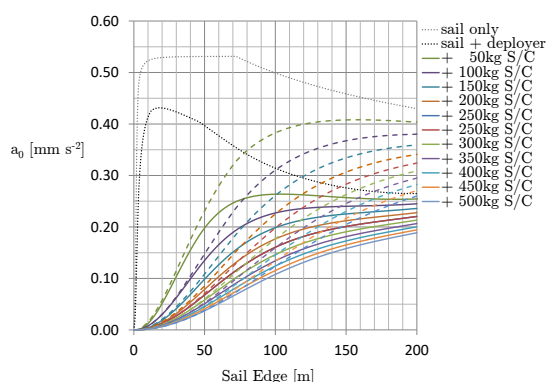


Figure 11: Characteristic acceleration for different additional space craft (S/C) mass. Dashed lines for Gossamer-1 with deployment units that can be jettisoned (no mechanism mass for the sail craft). Solid lines show the characteristic acceleration for a system with central deployer that stays on the sail craft after deployment.

Due to the consideration of the mass scaling laws, the functions for the characteristic acceleration do not approach the limit defined by the membrane density. Such results were shown in previous studies e.g. by Seefeldt (2018) and Grundmann et al. (2019a) based on a sail membrane of $7.5\mu\text{m}$ thickness. Here, the additional mass required for the booms when the sail gets larger and larger can even lead to a reduction of the characteristic acceleration with increasing sail size. For small space craft masses we find an optimal size while for larger spacecraft mass it only tends to a limit value.

When comparing the two designs (jettisoned deployment units or fixed central deployer), it can be seen that for sail up to 50 m side length the difference between the two designs with respect to the achievable characteristic acceleration is small, while for larger sails it becomes significant. For lighter additional spacecraft masses, this effect is more pronounced.

6. Mission applications

Besides the sail itself a fully functional sailcraft requires a bus system. The bus system mass of the technology demonstrator Gossamer-1 would have been about 10 kg. For an estimate it is assumed that the sail attitude control system and deep-space communication equipment add another 20 kg. In addition 10 kg of science instruments and 10 kg for a nanolander like MASCOT (see Ho et al. (2016a)) or MASCOT2 (see Ho et al. (2016b)) leaves us with a 50 kg mass in addition to the sail itself. Considering multiple landers and/or margins for bus systems, an additional mass of 50 kg to 100 kg can be expected. Following the bus + payload trace in Figure 11 it is found that a $50\text{m} \times 50\text{m}$ already yield characteristic accelerations a_c between 0.125mm s^{-2} and 0.2mm s^{-2} .

In studies carried out alongside to DLR’s Gossamer-1 developments (see Spietz et al. (2021)) the following three missions were identified and studied over a period of two years by the three Gossamer Science Working Groups. Each was presented in a comprehensive peer-reviewed paper.

6.0.1. Multiple Near-Earth Asteroid Rendezvous

Dachwald et al. (2014) presented a multiple near-Earth object (NEO) rendezvous (MNR) and fly-by mission to visit and rendezvous for at least several rotation periods of the respective object with at least three significant near-Earth asteroids (NEA) out of a pre-selected population, and to perform faster fly-bys at additional other NEOs within the set lifetime of a decade. MNR performance of optimized solar sails have been studied more extensively since, e.g. Pelsoni et al. (2016). “Slow” sails with a characteristic acceleration of $a_c < 0.2\text{mm s}^{-2}$ were studied in the context of the asteroid mitigation tabletop exercise conducted bi-annually at the IAA Planetary Defense Conference (PDC). For the PDC 2017, it was demonstrated that the re-targeting capability shown by Pelsoni et al. (2016) for solar sails of $a_c = 0.2\text{mm s}^{-2}$ also exists for surprise targets in an ongoing mission. This corresponds to sail sizes for initial missions based on deployment strategies optimized for solar sailing, i.e. using jettisoned deployment units. Grundmann et al. (2019a) For the PDC 2019 “slow” sails of small size or based on ad-hoc re-used technologies from other membrane deployment applications were analyzed, with encouraging results for early low-cost sail missions. MNR capability is achieved already at $a_c < 0.1\text{mm s}^{-2}$ and single NEA rendezvous (SNR) is feasible from $a_c = 0.06\text{mm s}^{-2}$ with a choice of 2 to 3

SNR targets per launch date. Grundmann et al. (2021); Ceriotti et al. (2021)

Re-targeting of fictitiously on-going missions to the exercise target asteroid was again considered. Grundmann et al. (2019b) These studies followed up on earlier re-use oriented concepts. Grundmann et al. (2015) For comparison, the as of this writing ongoing sample-return missions of the solar-electric propelled (SEP) HAYABUSAS and OSIRIS-REX are effectively of the SNR-plus-fly-by type, including Earth itself as a “NEO” for the fast fly-by to drop the sample capsule. SEP MNR missions have been studied, e.g. SESAME Maiwald and Marchand (2013) which required a total Δv of 16.6 km s^{-1} to rendezvous with 5 NEAs selected solely on the basis of trajectory optimization. The 1571 kg SESAME design, only slightly larger than Dawn, carried 55 kg of science payload including 5 small, 4.3 kg landers, similar to our sail-based MNR studies. Sails with an a_c between 0.1 and 0.3 mm s^{-2} have been considered “first-generation” sails, also in the studies previously mentioned. Thus, it appears that a “0th generation” sail of a performance similar to this study could already compete with state-of-the-art of SEP NEA rendezvous missions.

6.0.2. Displaced L_1

McInnes et al. (2014) presented a spaceweather early warning mission stationkeeping with Earth ahead of the Sun-Earth Lagrange point L_1 towards the Sun, using the sail thrust to augment Earth’s gravity in the balance of orbital forces to generate an artificial Displaced L_1 point (DL1), and carrying a very lightweight suite of plasma instruments. The DL1 position was expected and required to at least double the warning time for oncoming solar storms which can disturb power grids, knock out spacecraft services, hinder radio communication, and increase high altitude radiation on Earth. This DL1 position was to be maintained for 10 years, at least. This mission is infeasible for chemical L_1 -displacement-sustaining propulsion and SEP would only enable a short mission duration of a few years. The 10-year mission duration based on the highly successful ACE and SOHO missions requires an effective Δv of nearly 95 km s^{-1} . The DL1 sailcraft was in many ways considered the least challenging of the three Gossamer Reference Mission Studies because it had the most modest performance requirement at $a_c = 0.3 \text{ mm s}^{-2}$, the most tranquil trajectory in terms of attitude control agility, and the most benign environment, continuously operating near Earth. Also, sail degradation during the mission would not lead to loss of stationkeeping nor an abrupt mission end, merely the displacement distance

ahead of L_1 would recede gradually and in proportion back towards the purely ballistic L_1 region of halo orbits.

6.0.3. Solar Polar Orbiter

Macdonald et al. (2014) presented a Solar Polar Orbiter (SPO) for which the solar sail is used to raise the inclination of its heliocentric orbit much further than possible by gravity-assist fly-bys, chemical or electrical propulsion combined. The Solar Polar Orbiter (SPO) mission was the most challenging mission among the Gossamer Reference Mission Studies with respect to its a_c requirements with performances in the range of $a_c > 0.29 \dots 0.54 \text{ mm s}^{-2}$. The additional spacecraft mass was in the range of 45 to 305 kg for science payloads between 5 and 40 kg. This is beyond the capabilities of sailcraft using a central deployment unit that cannot be jettisoned and a $5 \mu\text{m}$ membrane (solid lines in Figure 11) except for the very lightest payloads and when a significantly longer flight time or/and not fully polar orbit is accepted. This may well be acceptable considering that multiple gravity assist supported and SEP based SPO concepts can not reach comparable inclinations and proximity to the Sun.

6.0.4. Space Situational Awareness and Space Debris

The three mission classes discussed in the preceding sections are all linked to space situational awareness (SSA). Directly for DL_1 mission, for MNR by the incorporation of planetary defence related efforts in the SSA activities of many space agencies, and for SPO there is a link to SSA applications through science of the Sun and the heliosphere. However, these are not all applications of solar sails in SSA, just the most uniquely feasible that were identified in a broad search by the Gossamer Science Working Groups.

A further useful mission in the SSA context could arise from the unique combination of features of an early, small and/or non-optimized technology demonstration sail craft in Earth orbit. Between the envisaged size and performance of Gossamer-2 and Gossamer-3, it would be highly suited to map the natural and artificial debris environment in the Earth-Moon system. Grundmann et al. (2015, 2019b) So far, all space debris sensors in Earth orbit have been deployed on ballistic orbits only subject to natural atmospheric decay. Using a solar sail, it becomes possible to map the entire cis-lunar space by slowly spiralling out with a very large detector area – the membrane itself. While many dust detector technologies can be integrated on relatively thin membranes, the SOLID technology developed at DLR Bremen integrates with photovoltaic panels (see

Bauer et al. (2017)). The photovoltaic panels can be membrane-based, like GoSOLAR, or conventional rigid structures. Membrane-based arrays can offer a larger area. This also opens the secondary use as debris detectors of future large photovoltaic arrays of future space tugs which frequently traverse a wide range of orbits. With the recent imaging of the Kordylewski clouds near the Earth-Moon system's L_4 and L_5 stable points Slíz-Balogh et al. (2018, 2019); Laufer et al. (2007); Kordylewski (1961), an additional planetary science case has appeared for this mission taking interest in two unique celestial objects shaped by orbital dynamics in the Earth-Moon-Sun system as well as solar radiation pressure. A "slow" sail has the advantage of longer dust counter integration time within a specific region that would be passed faster by a high-performance sail. Thus, it would be an ideal mission for early sails, of relatively small area or technology re-use based designs. It would be possible to combine a space debris survey of this kind with plasma and radiation measurements, in particular when at the same time characterizing new photovoltaic technologies as envisaged for GoSOLAR in a controlled study of plasma-related space weathering effects.

7. Discussion and Conclusion

The analysis of the proposed boom and central deployment unit for a solar-sail application shows that scaling limits dominate the efficiency of the design in the small-size region. Proper selection of key components such as booms and membrane and an appropriate stowing and deployment strategy is key to realizing mass efficient solar sails below 10 m edge length. In the mid-size region up to 50 m edge length a minimum in area mass of the sail is reached with rather good mass specific performances. However, for even larger sails the area mass increases again. Here low fundamental frequency requirements applied to the stowed system and a lightweight sail shows a high effect on the performance. Hence for large sail it is of high importance to minimize launch load design requirements and select sail architectures that induce small structural loads to the underlying support structure.

In order to maximize the characteristic acceleration, especially for very large sails, it is a clear advantage if the mass of the deployment mechanisms can be jettisoned and thus no longer contribute to the sail craft mass. This was of course the motivation within the Gossamer-1 project. However, considering that candidates for first missions do not require such large sails

and that also the Gossamer-1 project considered up-scaling only up to 50 m the gained additional characteristic acceleration is small while it is a dearly bought advantage. It comes at the expense of additional complexity as well as an increase of launch mass and volume.

To picture this more clearly, each jettisoned deployment unit has about the mass and volume of the central deployer. So the question is if it can be justified to increase the deployment mechanisms size and volume by the factor of four in order to gain an increase of the characteristic acceleration of the sail craft. As explained above the complexity of a deployment unit is comparable to the one of a CubeSat, which means that besides the main spacecraft four additional small spacecraft with deployment mechanisms have to function until the deployment is completed. This certainly increases possible point of failures and thereby the risk of an unsuccessful deployment.

In principle the additional complexity and possible risks can be counteracted with more project resources (e.g. built-in redundancies, implement sophisticated integration and testing processes). The same applies for the increase in launch mass and volume which increases launch costs. Unfortunately at the moment solar sail projects are often relatively low funded which makes these disadvantages even more severe. For instance it can be stated that this was one problem for the Gossamer-1 activity when it came to hardware implementation. With the resources available it was possible to build a qualification model of one deployment unit and run a qualification test campaign, but implementing four units in addition to the spacecraft bus was out of reach.

With the above reasoning it is concluded that for square solar sails up to 50 m edge length, based on coilable CFRP booms in a crossed configuration, a central deployer is the reasonable choice. Such a solar sail would also be sufficient for the implementation of first solar sail missions, e.g. flying to near-Earth objects.

References

- Bauer, W., Braukhane, A., Grundmann, J.T., Romberg, O., Danne- mann, F., Barschke, M., 2017. Step by step realization of an operational on orbit detection network, in: Proceedings of the 7th European Conference on Space Debris, ESA Space Debris Office, Noordwijk. URL: <https://elib.dlr.de/118576/>.
- Cerioti, M., Viavattene, G., Moore, I., Peloni, A., McInnes, C.R., Grundmann, J.T., 2021. Sailing at the brink - the no-limits of near-/now-term-technology solar sails and sep spacecraft in (multiple) neo rendezvous. Advances in Space Research, Solar Sailing: Concepts, Technology, and Missions II .

- Dachwald, B., Boehnhardt, H., Broj, U., Geppert, U.R., Grundmann, J.T., Seboldt, W., Seefeldt, P., Spietz, P., Johnson, L., Kührt, E., et al., 2014. Gossamer roadmap technology reference study for a multiple neo rendezvous mission, in: Macdonald, M. (Ed.), *Advances in Solar Sailing*. Springer, Berlin Heidelberg, pp. 211–226. URL: https://doi.org/10.1007/978-3-642-34907-2_15.
- Greschik, G., Murphey, T., Mikulas, M., Belvin, W., 2003. A rule of thumb for the suspension of film sheets without catenaries, in: 44th AIAA/ASME/ASCE/AHS/ASC Structures, Structural Dynamics, and Materials Conference, p. 1907. URL: <https://doi.org/10.2514/6.2003-1907>.
- Grundmann, J.T., Bauer, W., Biele, J., Boden, R., Ceriotti, M., Cordero, F., Dachwald, B., Dumont, E., Grimm, C.D., Herčík, D., Ho, T.M., Jahnke, R., Koch, A.D., Koncz, A., Krause, C., Lange, C., Lichtenheldt, R., Maiwald, V., Mikschl, T., Mikulz, E., Montenegro, S., Pelivan, I., Peloni, A., Quantius, D., Reershemius, S., Renger, T., Riemann, J., Ruffer, M., Sasaki, K., Schmitz, N., Seboldt, W., Seefeldt, P., Spietz, P., Spröwitz, T., Sznajder, M., Tardivel, S., Tóth, N., Wejmo, E., Wolff, F., Ziach, C., 2019a. Capabilities of gossamer-1 derived small spacecraft solar sails carrying mascot-derived nanolandings for in-situ surveying of NEAs. *Acta Astronautica* 156, 330–362. URL: <https://doi.org/10.1016/j.actaastro.2018.03.019>.
- Grundmann, J.T., Bauer, W., Biele, J., Cordero, F., Dachwald, B., Koncz, A., Krause, C., Mikschl, T., Montenegro, S., Quantius, D., Ruffer, M., Sasaki, K., Schmitz, N., Seefeldt, P., Toth, N., Wejmo, E., Koch, A., Seboldt, W., Sznajder, M., 2015. From sail to soil - getting sailcraft out of the harbour on a visit to one of earth's nearest neighbours, in: Ailor, W., Tremayne-Smith, R. (Eds.), 4th IAA Planetary Defense Conference – PDC 2015, IAA on-line. URL: <https://elib.dlr.de/103048/>.
- Grundmann, J.T., Bauer, W., Boden, R., Ceriotti, M., Chand, S., Cordero, F., Dachwald, B., Dumont, E., Grimm, C.D., Herčík, D., Hérique, A., Ho, T.M., Jahnke, R., Kofman, W., Lange, C., Lichtenheldt, R., McInnes, C., Meß, J.G., Mikschl, T., Mikulz, E., Montenegro, S., Moore, I., Pelivan, I., Peloni, A., Plettemeier, D., Quantius, D., Reershemius, S., Renger, T., Riemann, J., Rogez, Y., Ruffer, M., Sasaki, K., Schmitz, N., Seboldt, W., Seefeldt, P., Spietz, P., Spröwitz, T., Sznajder, M., Tóth, N., Viavattene, G., Wejmo, E., Wiedemann, C., Wolff, F., Ziach, C., 2021. Responsive integrated small spacecraft solar sail and payload design concepts and missions. *Advances in Space Research, Solar Sailing: Concepts, Technology, and Missions II*.
- Grundmann, J.T., Bauer, W., Boden, R., Ceriotti, M., Chand, S., Cordero, F., Dachwald, B., Dumont, E., Grimm, C.D., Herčík, D., Hérique, A., Ho, T.M., Jahnke, R., Kofman, W., Lange, C., Lichtenheldt, R., McInnes, C., Mess, J.G., Mikschl, T., Mikulz, E., Montenegro, S., Moore, I., Pelivan, I., Peloni, A., Plettemeier, D., Quantius, D., Reershemius, S., Renger, T., Riemann, J., Rogez, Y., Ruffer, M., Sasaki, K., Schmitz, N., Seboldt, W., Seefeldt, P., Spietz, P., Spröwitz, T., Sznajder, M., Tóth, N., Viavattene, G., Wejmo, E., Wiedemann, C., Wolff, F., Ziach, C., 2019b. Responsive exploration and asteroid characterization through integrated solar sail and lander development using small spacecraft technologies, in: *Presentations of the 6th IAA Planetary Defense Conference*. URL: <http://pdc.iaaweb.org/>.
- Grundmann, J.T., Hillebrandt, M., Leipold, M., Seefeldt, P., Sickinger, C., Spietz, P., 2019c. Solar sail development and testing history in Germany from Oberth to the Gossamer-1 qm, in: *Presentations of the 5th International Symposium on Solar Sailing*. URL: <http://iss2019.org/>.
- Hillebrandt, M., 2019. *Conceptual Design of Deployable Space Structures* (accepted, in press). Ph.D. thesis. Technical University Carolo Wilhelmina, Braunschweig, Germany. URL: <https://elib.dlr.de/134661/>.
- Hillebrandt, M., Meyer, S., Zander, M., Straubel, M., Hühne, C., 2014. The boom design of the de-orbit sail satellite, in: *European Conference on Spacecraft Structures, Materials and Mechanical Testing*. URL: <https://elib.dlr.de/95684/>.
- Hillebrandt, M., Zander, M., Hühne, C., 2019. Sliding core deployment mechanism for solar sails based on tubular shell masts, in: *5th International Symposium on Solar Sailing*. URL: <https://elib.dlr.de/129630/>.
- Hillebrandt, M., Zander, M.E., 2018. Conceptual design of the deployable booms for the gosolar-satellite, in: *European Conference on Spacecraft Structures, Materials and Environmental Testing*. URL: <https://elib.dlr.de/134661/>.
- Ho, T.M., Baturkin, V., Grimm, C., Grundmann, J.T., Hobbie, C., Ksenik, E., Lange, C., Sasaki, K., Schlotterer, M., Talapina, M., Termtanasombat, N., Wejmo, E., Witte, L., Wrasmann, M., Wübbels, G., Röbber, J., Ziach, C., Findlay, R., Biele, J., Krause, C., Ulamec, S., Lange, M., Mierheim, O., Lichtenheldt, R., Maier, M., Reill, J., Sedlmayr, H.J., Bousquet, P., Bellion, A., Bompis, O., Cenac-Morthe, C., Deleuze, M., Fredon, S., Jurado, E., Canalias, E., Jaumann, R., Bibring, J.P., Glassmeier, K.H., Hercik, D., Grott, M., Celotti, L., Cordero, F., Hendrikse, J., Okada, T., 2016a. MASCOT—The Mobile Asteroid Surface Scout Onboard the Hayabusa2 Mission. *Space Science Reviews* 208, 339–374. URL: <http://dx.doi.org/10.1007/s11214-016-0251-6>.
- Ho, T.M., Lange, C., Grimm, C., Thimo Grundmann, J., Röbber, J., Schröder, S., Skoczylas, T., Ziach, C., Biele, J., Cozzoni, B., Krause, C., Kuchemann, O., Maibaum, M., Ulamec, S., Lange, M., Mierheim, O., Maier, M., Herique, A., Team, M.S., 2016b. A Mobile Asteroid Surface Scout for the AIDA Mission, in: *Presentations of the EGU General Assembly, Vienna Austria*.
- Kordylewski, K., 1961. Photographische untersuchungen des librationpunktes 15 im system erde-mond. *Acta Astronomica* 11, 165–168.
- Laufer, R., Tost, W., Zeile, O., Srama, R., Roeser, H.P., 2007. The Kordylewski clouds – an example for a cruise phase observation during the lunar mission bw1, in: *Proceedings of the 11th ISU Annual International Symposium*, pp. 21–23.
- Macdonald, M., McGrath, C., Appourchaux, T., Dachwald, B., Finstlerle, W., Gizon, L., Liewer, P.C., McInnes, C.R., Mengali, G., Seboldt, W., Sekii, T., Solanki, S.K., Velli, M., Wimmer-Schweingruber, R.F., Spietz, P., Reinhard, R., 2014. Gossamer roadmap technology reference study for a solar polar mission, in: Macdonald, M. (Ed.), *Advances in Solar Sailing*. Springer, Berlin Heidelberg, pp. 243–257. URL: https://doi.org/10.1007/978-3-642-34907-2_17.
- Maiwald, V., Marchand, E., 2013. Sesame opens: A precursor to human asteroid missions, in: *Proceedings of the International Astronautical Congress*. URL: <https://elib.dlr.de/84842/>.
- McInnes, C.R., Bothmer, V., Dachwald, B., Geppert, U.R.M.E., Heiligers, J., Hilgers, A., Johnson, L., Macdonald, M., Reinhard, R., Seboldt, W., Spietz, P., 2014. Gossamer roadmap technology reference study for a sub-11 space weather mission, in: Macdonald, M. (Ed.), *Advances in Solar Sailing*. Springer, Berlin Heidelberg, pp. 227–242. URL: https://doi.org/10.1007/978-3-642-34907-2_16.
- Murphey, T.W., 2006. *Recent Advances in Gossamer Spacecraft, Chapter 1 Booms and Trusses*, ISBN-13: 978-1563477775. American Institute of Aeronautics and Astronautics, Reston.
- Peloni, A., Ceriotti, M., Dachwald, B., 2016. Solar-sail trajectory design for a multiple near-earth-asteroid rendezvous mission. *Journal of Guidance, Control, and Dynamics* 39, 2712–2724. URL: <https://doi.org/10.2514/1.G000470>.
- Rubin, C.P., 1969. Deployable boom. US Patent 3,434,254.
- Seefeldt, P., Dachwald, B., 2021. Temperature increase on folded solar sail membranes. *Advances in Space Research, Solar Sailing:*

- Concepts, Technology, and Missions II .
- Seefeldt, P., 2017. A stowing and deployment strategy for large membrane space systems on the example of gossamer-1. *Advances in Space Research* 60, 1345–1362. URL: <https://doi.org/10.1016/j.asr.2017.06.006>.
- Seefeldt, P., 2018. Development and Qualification of Deployable Membranes for Space Applications. Ph.D. thesis. Universität Bremen. URL: <https://elib.suub.uni-bremen.de/edocs/00106591-1.pdf>.
- Seefeldt, P., Spietz, P., Sproewitz, T., Grundmann, J.T., Hillebrandt, M., Hobbie, C., Ruffer, M., Straubel, M., Tóth, N., Zander, M., 2017. Gossamer-1: Mission concept and technology for a controlled deployment of gossamer spacecraft. *Advances in Space Research* 59, 434–456. URL: <https://doi.org/10.1016/j.asr.2016.09.022>.
- Sickinge, C., 2009. Verifikation entfaltbarer composite-booms für gossamer-raumfahrtsysteme. Ph.D. thesis. Technische Universität Carolo-Wilhelmina zu Braunschweig. Shaker, Aachen, ISBN: 9783832280499.
- Slíz-Balogh, J., Barta, A., Horváth, G., 2018. Celestial mechanics and polarization optics of the kordylewski dust cloud in the earth–moon lagrange point l5–part i. three-dimensional celestial mechanical modelling of dust cloud formation. *Monthly Notices of the Royal Astronomical Society* 480, 5550–5559. URL: <https://doi.org/10.1093/mnras/sty3099>.
- Slíz-Balogh, J., Barta, A., Horváth, G., 2019. Celestial mechanics and polarization optics of the kordylewski dust cloud in the earth–moon lagrange point l5–part ii. imaging polarimetric observation: new evidence for the existence of kordylewski dust cloud. *Monthly Notices of the Royal Astronomical Society* 482, 762–770.
- Spietz, P., Spröwitz, T., Seefeldt, P., Grundmann, J.T., Jahnke, R., Mikschl, T., Mikulz, E., Montenegro, S., Siebo, R., Renger, T., Ruffer, M., Sasaki, K., Sznajder, M., Tóth, N., Ceriotti, M., Dachwald, B., McInnes, C., Seboldt, W., Dumont, E., Quantius, D., Riemann, J., Bauer, W., Wiedemann, C., Boden, R., Cordero, F., Grimm, C.D., Herčík, D., Ho, T.M., Lange, C., Lichtenheldt, R., Schmitz, N., Wejmo, E., Wolff, F., Ziach, C., Chand, S., Hérique, A., Kofman, W., Meß, J.G., Moore, I., Pelivan, I., Peloni, A., Plettemeier, D., Rogez, Y., Viavattene, G., 2021. Paths not taken – the gossamer roadmap’s other options. *Advances in Space Research, Solar Sailing: Concepts, Technology, and Missions II* .